*Malaysian Journal of Chemistry, 2022, Vol. 24(2), 250-257*
(Special Issue: International Conference on Synthesis Chemistry-ICOSC2022, Universiti Teknologi MARA)

# Synthesis, Characterization, DFT and Antibacterial Screening of Schiff Base Derived from Isatin with Thiocarbohydrazide and Their Cu(II) And Zn(II) Complexes

**Ummi Liyana Mohamad Rodzi[1], Karimah Kassim[2], Amalina Mohd Tajuddin[3], Muhamad Kamil Yaakob[1] and Nurul Aili Zakaria[1]**
[1]Faculty of Applied Sciences, Universiti Teknologi MARA, 40450 Shah Alam, Selangor, Malaysia
[2]Institute of Science, Universiti Teknologi MARA, 40450 Shah Alam, Selangor Malaysia
[3]Atta-ur-Rahman Institute for Natural Product Discovery (AuRIns), UiTM Puncak Alam, 42300 Bandar Puncak Alam, Selangor, Malaysia
*Corresponding authors (e-mail: ummi.liyana5158@gmail.com, karimah@uitm.edu.my)

A Schiff base ligand, *N*,2-bis(2-oxoindolin-3-ylidene)hydrazine-1-carbothiohydrazine (B1) was synthesized via condensation reaction of isatin and thiocarbohydrazide. The ligand was reacted with copper(II) acetate monohydrate and zinc(II) chloride producing *N*,2-bis(2-oxoindolin-3-ylidene)hydrazine-1-carbothiohydrazinecopper(II) (CuB1) and *N*,2-bis(2-oxoindolin-3-ylidene)hydrazine-1-carbothiohydrazinezinc(II) (ZnB1). The ligand structures and its together with copper and zinc complexes were characterized using elemental analysis, melting point, infrared spectroscopy, $^{1}$H and $^{13}$C Nuclear Magnetic Resonance spectroscopy and UV-Visible spectroscopy. In this study, the optimized structures of the compounds were calculated using the B3LYP hybrid function with a DNP basis set to evaluate the electronic properties of the compounds. The antibacterial screening using microtitre-plate assay was conducted against *Streptococcus mutans* Clarke (ATCC 700610) and *Staphylococcus aureus* subsp. *aureus* Rosenbach (ATCC 6538) and no significant activity were reported.

**Key words**: Antibacterial; density functional theory (DFT); isatin; optimization; thiocarbohydrazide

*Received: March 2022; Accepted: March 2022*

Schiff bases have played a vital role in developing coordination chemistry due to their excellent chelating ability as they are readily form stable complexes with various metal ions. One such is isatin. Isatin was first isolated from the oxidation product of indigo from nitric and chromic acids by Erdmann and Laurent [1]. Isatin has been reported to possess many biological properties such as, antibacterial [2, 3, 4], anticancer [5, 6], antituberculosis [7] and antiviral [8, 9]. Various functional groups and their electronic characteristics have given isatin the ability to exhibit biological properties. Thiocarbohydrazone, which is another important class of organic chemistry, aids the coordination process via azomethine nitrogen and sulfur [10]. The synthesis of Schiff base containing isatin and thiocarbohydrazide with its subsequent antitumor activity against Ehrlich ascites carcinoma in Swiss albino mice have been reported earlier [11]. Therefore, this study aims to further discover and determine the electronic properties of *N*,2-bis(2-oxoindolin-3-ylidene)hydrazine-1-carbothiohydrazine (B1), *N*,2-bis(2-oxoindolin-3-ylidene)hydrazine-1-carbothiohydrazinecopper(II) (CuB1) and *N*,2-bis(2-oxoindolin-3-ylidene)hydrazine-1-carbothiohydrazine-zinc(II) (ZnB1) using density functional theory (DFT) calculations as well as the antibacterial screening of the synthesized compounds against two bacterial strains, *Streptococcus mutans* Clarke (ATCC 700610) *(S.mutans)* and *Staphylococcus aureus* subsp. *aureus* Rosenbach (ATCC 6538) *(S.aureus)*. Both gram positive bacteria have been chosen to be tested because they have increasingly become the main causes of infections among the community [12]. Scheme 1 shows the proposed synthetic route of synthesizing ligand B1 and metal complexes.

## MATERIAL AND METHODS

### 1. Materials

Isatin, thiocarbohydrazide, copper(II) acetate mono-hydrate, zinc(II) chloride, absolute ethanol and all other reagents were used without further purification and commercially available from Sigma Aldrich.

### 2. Physical Measurements

Elemental analyses (carbon, hydrogen, nitrogen and sulfur) were performed on Thermo Finnigan Flash EA 110 Elemental Analyzer. Infrared (IR) spectra were recorded using KBr pellets on Perkin Elmer 1600 Spectrometer at 400 – 4000 cm$^{-1}$. $^{1}$H and $^{13}$C NMR

†Paper presented at the International Conference on Synthesis Chemistry-ICOSC2022, Universiti Teknologi MARA

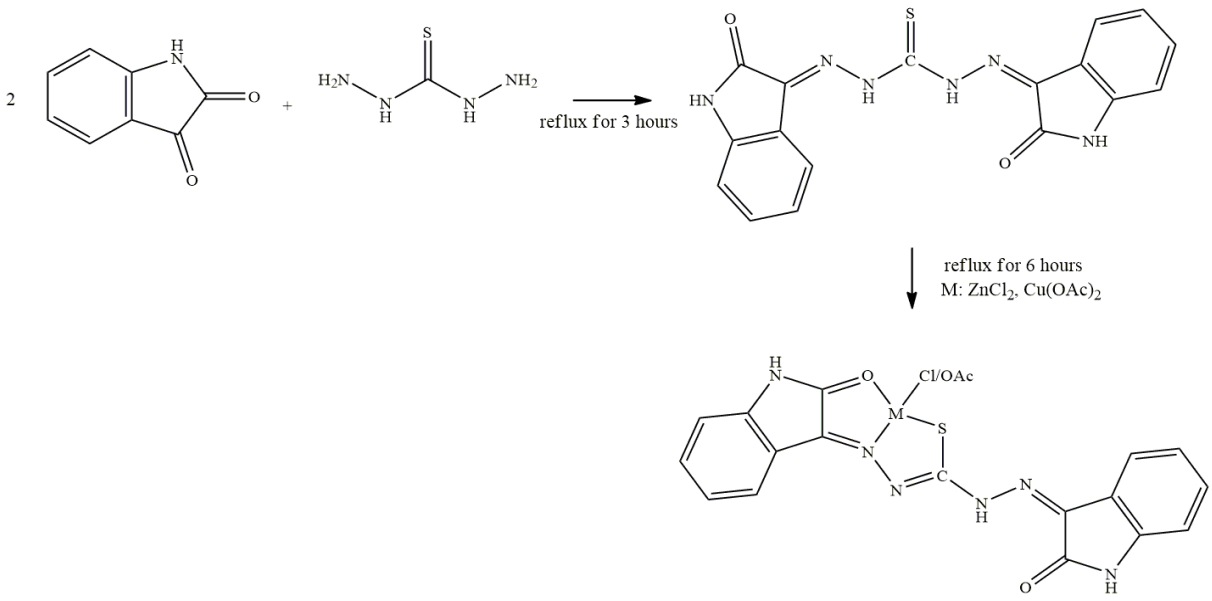


**Scheme 1.** Synthesis of *N*,2-bis(2-oxoindolin-3-ylidene)hydrazine-1-carbothiohydrazine (B1) and its complexes.

spectra of the ligand and zinc(II) complex were recorded using Bruker Varian Spectrometer at 500 MHz in deuterated dimethyl sulfoxide (DMSO-$d_6$). UV-Visible spectra were obtained from Perkin Elmer UV-Vis Lambda 35 using acetonitrile (MeCN) solution in a quartz cell. All measurements were carried out at room temperature.

### 3. Synthesis of B1

The method for the synthesis of the ligand refers to [11] with some modifications. The ligand was prepared by dissolving isatin and thiocarbohydrazide into hot absolute ethanol (30 mL) and the reaction mixture was refluxed for three hours. The yellow precipitate formed was filtered off, washed with cold ethanol and air dried overnight. The remaining filtrate was left for recrystallization.

### 4. Synthesis of ZnB1 and CuB1

The ligand and zinc(II) chloride were dissolved in a hot ethanolic solution (30 mL). 1 mL of triethylamine was added into the solution and refluxed for 6 hours. The red solution was cooled to room temperature, filtered and washed with cold ethanol forming a solid red powder. The powder was air-dried overnight. The steps were repeated by replacing zinc(II) chloride with copper(II) acetate monohydrate.

### 5. Computational Details

Theoretical studies were made based on density functional theory (DFT) calculations using BIOVIA Material Studio DMol$^3$ with Becke's three-parameter hybrid functional (B3) for the exchange and Lee, Yang and Parr (LYP) correlation functional [13]. The basis set used in the study is the double numerical with polarisation (DNP) function. This type of basis set is acknowledged to be comparable basis set to the 6-31G** Gaussian [14].

### 6. Microtiter Plate Assay for Antibacterial Screening

The microtiter plate assay method was used in the antibacterial screening according to [15]. Anti-bacterial screening for the synthesized compounds was evaluated against the *Staphylococcus aureus* subsp. *aureus* Rosenbach (ATCC 6538) and *Streptococcus mutans* Clarke (ATCC 700610). The bacterial glycerol stocks were obtained from Natural Approach to Oral Health (NatOH) research initiative group, Faculty of Dentistry, UiTM. The glycerol stock was inoculated in 5 mL Trypticase Soy broth for *S. aureus* ATCC 6538 and Brain Heart Infusion broth for *S. mutans* ATCC 700610. The bacteria were grown for 24 hours at 37 °C. The overnight inoculum was later streaked onto each corresponding agar plate to select the single colonies for the antibacterial assay. The isolated colonies of microorganisms were cultured in Mueller Hinton Broth (MHB) and placed in an incubator shaker for 24 hours at 37 °C. The overnight grown microorganisms were adjusted to a standardized final $OD_{625nm}$ of approximately 0.08-0.10, which is equivalent to $10^8$ CFU/mL. Further dilution was done using sterile MHB to achieve a final concentration of $5x10^5$ CFU/mL. Samples, Ampicillin (positive control) and DMSO (negative control) were prepared accordingly to achieve final concentration of 10 mg/mL. Next, the samples together with the controls were made triplicates and loaded into the wells. The plates were covered and incubated for 24 hours at 37 °C. The results were determined visually by

observing the turbidity of the wells. For further confirmation on the presence of bacteria, the samples from the well were streaked onto the agar for the next 24 hours.

## RESULTS AND DISCUSSION

### 1. Physicochemical Data Analysis

The physical characteristics of the B1 ligand and its metal complexes are tabulated in Table 1. Elemental analyses of carbon, hydrogen, sulfur and nitrogen were performed to determine the elemental content of the synthesized compounds.

The elemental analyses data were acceptable within the calculated values. The melting point of the complexes was recorded to be higher than that of the ligand, likely being attributed to increase in molecular size and the presence of stronger dative covalent and ionic bonds [16].

**Table 1.** Physicochemical data of B1 ligand and metal complexes.

| Compounds | Colour | Percent Yield (%) | Chemical Formula | Melting Point (°C) | Elemental Analysis % Calculated (Found) | | | |
|---|---|---|---|---|---|---|---|---|
| | | | | | C | H | N | S |
| B1 | Yellow | 91.46 | $C_{17}H_{12}N_6O_2S$ | 281.7 | 56.04 (55.38) | 3.32 (3.58) | 23.06 (22.46) | 8.80 (7.03) |
| ZnB1 | Red | 64.77 | $C_{17}H_{11}ClN_6O_2SZn$ | 380.9 | 43.99 (43.91) | 2.39 (3.24) | 18.10 (17.86) | 6.91 (5.90) |
| CuB1 | Black | 85.78 | $C_{19}H_{18}CuN_6O_6S$ | 290.0 | 43.73 (43.73) | 3.48 (3.09) | 16.10 (17.28) | 6.14 (6.07) |

### 2. Infrared Spectroscopy

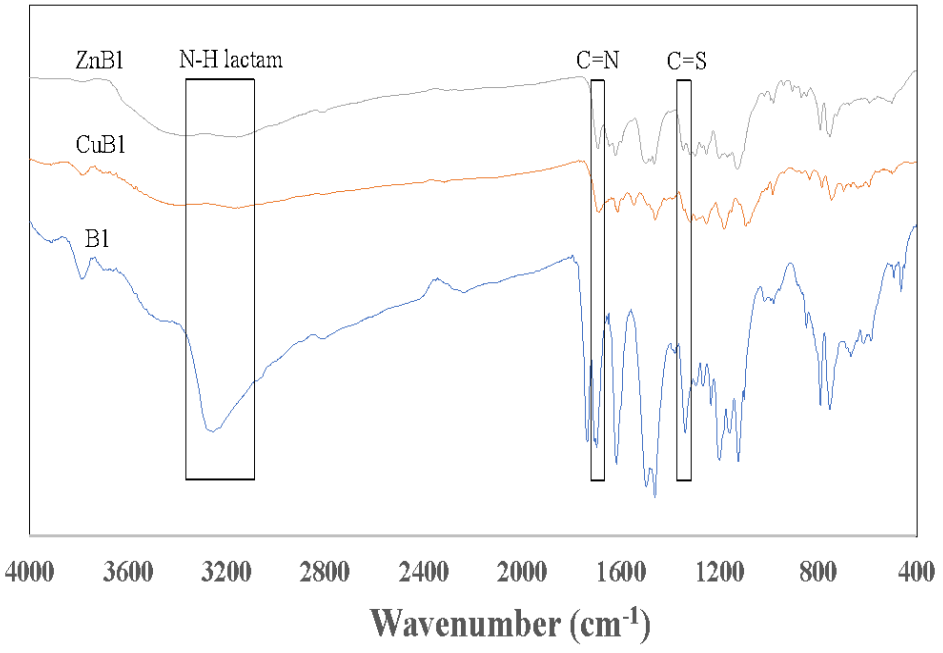


**Figure 1.** IR spectra of ligand and complexes.

The functional groups in the compounds were determined from infrared analysis. A strong stretching band was observed at 1697 $cm^{-1}$ indicating *v*(C=N) in the ligand spectrum [17]. This band shifts to a lower frequency for zinc(II) and copper(II) complexes at 1693 and 1691 $cm^{-1}$, respectively due to ligand coordination with the metal ions via azomethine nitrogen [18]. Meanwhile, the *v*(C=O) band for the ligand appeared at 1735 $cm^{-1}$ and completely disappears for zinc and copper(II) complexes. The absence of this band shows carbonyl oxygen of isatin might participated in the coordination of the metal ions. This is further supported by the stretching band around 1253 $cm^{-1}$ in both complexes attributed to *v*(C-O). The *v*(NH) of isatin moiety registers peaks in the range of 3254 $cm^{-1}$ for the ligand to 3160 and 3164 $cm^{-1}$ for CuB1 and ZnB1 indicating the nitrogen atom involve-ment in the coordination of complexes. Besides, the *v*(C=S) band at 1339 $cm^{-1}$ for the B1 ligand spectrum too shifts in the spectra of the complexes 1317 and 1347 $cm^{-1}$, respectively showing that the metal ion is coordinated via the sulfur atom.

## 3. $^{1}$H Nuclear Magnetic Resonance (NMR) Analysis

$^{1}$H NMR spectra of ligand and zinc complex were analyzed to elucidate each distinct type of hydrogen nuclei. CuB1 was not analyzed due to its para-magnetic property. Singlet peaks were observed near 12.94 and 11.34 ppm ascribed to NH thiocarbo-hydrazide and isatin NH, respectively. The aromatic protons of the isatin ring were observed at 7.60, 7.42, 7.14 and 6.98 ppm as multiplets. Similar peaks of aromatic protons were also observed for ZnB1. The aromatic protons were focused on the downfield region due to the ring current effect.

## 4. $^{13}$C Nuclear Magnetic Resonance (NMR) Analysis

The $^{13}$C NMR of B1 shows aromatic carbons in the region of 138.35 – 112.16 ppm. The signal for thione (C=S) appeared at 175.30 ppm while azomethine (C=N) and carbonyl carbon appeared at 162.55 and 138.50 ppm respectively. Meanwhile, for ZnB1, the signal for thione (C=S) which appeared around 178.5 ppm shifted to a higher range compared to the B1 ligand. For azomethine and carbonyl carbon, the peak appeared at the range of 164.0 ppm and 144.0 ppm. Thus, it can be deduced that there was participation of azomethine nitrogen, carbonyl oxygen and thione sulfur in the coordination of complexes and further supported for the data in infrared analysis [3].

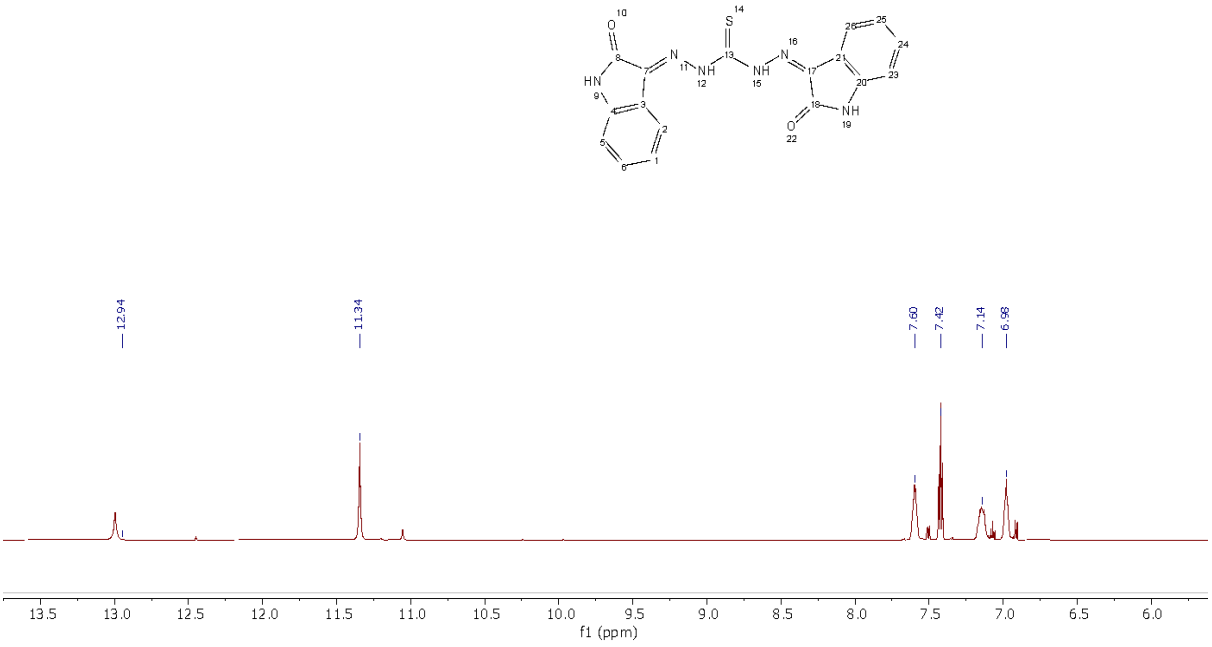


**Figure 2.** $^{1}$H NMR spectrum of B1.

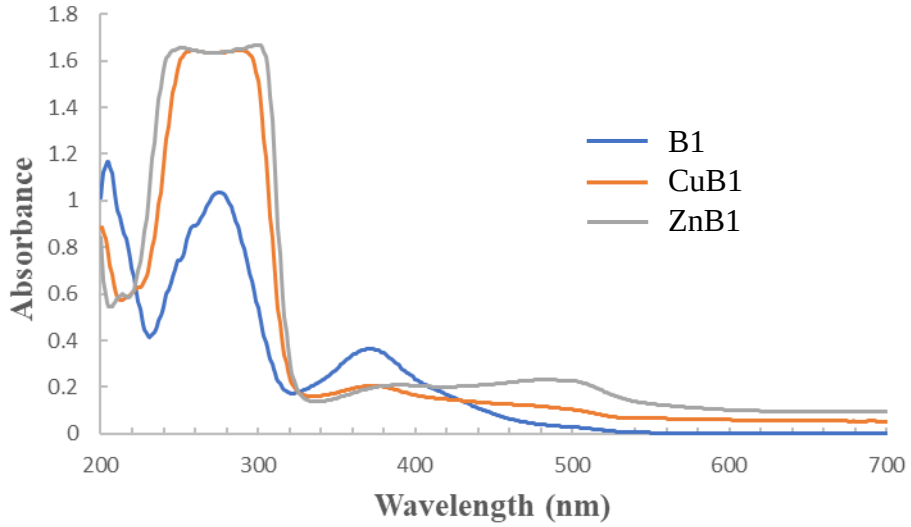


**Figure 3.** Absorption spectra of ligand and complexes.

## 5. UV-Visible Spectroscopy

Two absorption peaks were observed in the UV-Visible spectra of the ligand at the region of 249-274 nm and 372 nm ascribed as $\pi \rightarrow \pi^*$ and $n \rightarrow \pi^*$ transitions. The zinc and copper complexes spectra showed the ligand to metal charge transfer (LMCT) transition at 493 and 483 nm, respectively. This shift further supports the formation of the complexes [5].

## 6. Computational Analysis

### *6.1. Frontier Molecular Orbitals Analysis*

The relative structural stability of the ligand and both complexes were investigated using DFT calculations. One of the most important parameters of molecular electronic structure is Frontier Molecular Orbitals (FMO). The analysis of FMO can be used to evaluate the stability of the compounds [19]. Higher HOMO energy values indicate that the molecule is a good electron donor. Conversely, lower HOMO energy values show that the ability of the molecule to donate electrons is low. B3LYP method using DNP basis set of monomer form in the ground state was used to calculate the electron density of HOMO and LUMO [20].

As shown in Figure 4, the calculated molecular orbital unveiled that HOMO region for ligand and complexes are mainly distributed around the sulfur atom. In contrast, the LUMO region of the compounds delocalized around the azomethine group. The value of energy gap between the HOMO and LUMO for B1 ligand is 2.785 eV which can be considered to be almost similar with the value of analogous Schiff base (2.882 eV) reported previously [21]. The stability and reactivity of the compounds can be seen from the value of the energy gap. ZnB1 has the least energy gap compared to CuB1 and the B1 ligand. Thus, this indicates that ZnB1 may have lower stability, better conjugation and also rich in conductivity [22].

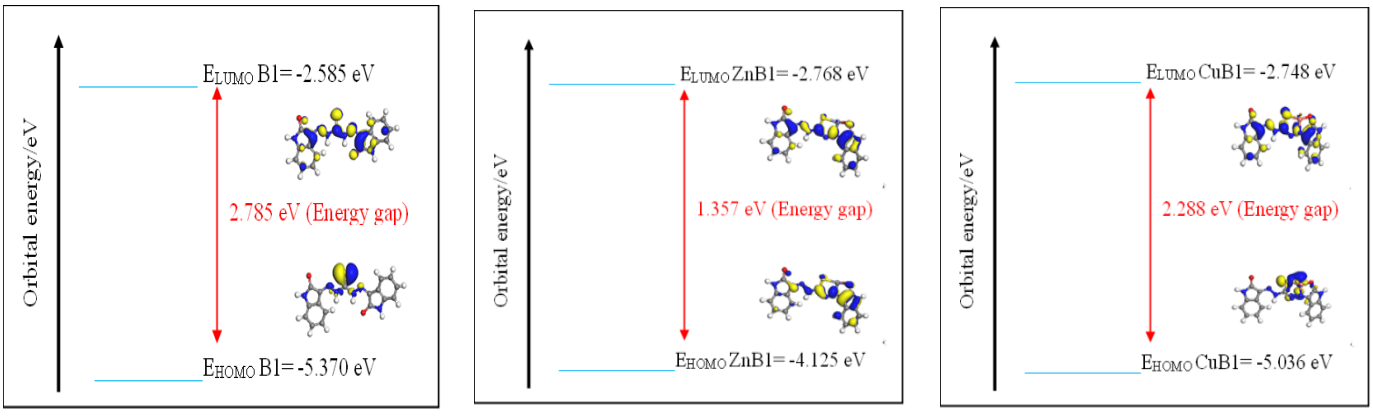


a) b) c)

**Figure 4.** The optimized molecular structure and HOMO-LUMO region of the compounds.

*6.2. Global Chemical Reactivity Descriptors (GCRD) Analysis*

$(\eta) = [(E_{LUMO} - E_{HOMO})/2]$ (Chemical hardness) (1)

$(S) = [1/2\eta]$ (Chemical softness) (2)

$(\mu) = [(E_{HOMO} + E_{LUMO})/2]$ (Chemical potential) (3)

*Electronegativity* $(\chi) = [(I + A)/2]$ (4)

*Electrophilicity* index $(\omega) = [\mu 2/2\eta]$ (5)

Maximum *additional* electric charge $(\Delta N_{max}) = [-\mu/\eta]$ (6)

Global Chemical Reactivity Descriptors (GCRD) method is one of the main techniques in analysing the chemical properties of compounds such as chemical potential, chemical hardness, electronegativity, electrophilicity index and chemical softness [23]. These properties can be calculated from the energies of frontier molecular orbitals [24]. The values of GCRD were calculated by using equation (1) to (6) as shown in Table 2.

The values of GCRD can be used to predict the relative reactivity of the compound. The ability of the compound to accept electrons is indicated by the value of chemical potential ($\mu$). The value of chemical potential is calculated using equation 3. Consequently, the least value of chemical potential that can be observed is 1.357 eV which indicates that ZnB1 has the highest electron acceptor ability. This is further supported with the electronegativity value that is calculated using equation 4 giving value of 3.447 eV. Chemical hardness ($\eta$) measures the change in chemical potential with electron density in distinct parts of the compound whereas chemical softness (S) is the contradiction [25]. By using equation 1 and equation 2, B1 has the highest value of chemical hardness ($\eta$) (1.393 eV) and lowest value of chemical softness (0.359 $eV^{-1}$). So, it can be said that B1 has the least tendency to exchange its electron cloud and has low polarizability effect. The electrophilicity index computes for the energy lowering of a B1 ligand due to maximal electron flow between donor and acceptor [24]. Strong electrophilicity index can be attributed to ZnB1 as it has the highest ability to accept electrons. Generally, organic compound can be classified as strong electrophile when it has value of $\omega$ exceeding 1.5 eV [26]. The maximum number of electrons ($\Delta N_{max}$) that can be accepted by the synthesized compounds were calculated using equation 6. It is found that ZnB1 has the highest value. Accordingly, based on the calculated GCRD parameters in Table 2, the results suggested that ZnB1 has the highest chemical reactivity.

## 7. Antibacterial Screening

The ligand and complexes possessed no antibacterial activity against *Streptococcus mutans* Clarke (ATCC 700610) and *Staphylococcus aureus* subsp. *aureus* Rosenbach (ATCC 6538). Triplicates of the ligand and complexes appeared cloudy in the 96 well plates, indicating the growth of bacteria. At the concentration set up, the synthesized compounds could not inhibit the growth of the bacteria, showing that there is no interaction between the molecule with the pathogen-specific protein in the bacteria [27]. Nonetheless, ampicillin, the positive control used during screening was susceptible to both bacteria strains, provided that the assay conducted was functional.

**Table 2.** Theoretically calculated reactivity descriptors.

| Compound | Chemical hardness, $\eta$ | Chemical softness, $S$ | Chemical potential, $\mu$ | Electronegativity, $\chi$ | Electrophilicity index, $\omega$ | $\Delta N_{max}$ |
|---|---|---|---|---|---|---|
| B1 | 1.393 | 0.359 | -3.978 | 3.978 | 5.680 | 2.856 |
| ZnB1 | 0.679 | 0.743 | -3.447 | 3.447 | 8.749 | 5.077 |
| CuB1 | 1.144 | 0.437 | -3.892 | 3.892 | 6.680 | 3.402 |

## CONCLUSION

In summary, *N*,2-bis(2-oxoindolin-3-ylidene) hydrazine-1-carbothiohydrazine and its complexes were synthesized with good yields of 65-91%. All the products were characterized using IR, $^{1}$H NMR, $^{13}$C NMR, elemental analyses and UV-Visible Spectroscopy. DFT/B3LYP/DNP method was used for the theoretical calculations. The calculations showed that ZnB1 has the highest reactivity compared to the B1 and CuB1. Therefore, ZnB1 exhibits the potential to be applied to corrosion-based studies for its richness in conductivity. However, all the synthesized compounds showed no significant antibacterial activity.

## ACKNOWLEDGEMENT

The authors wish to thank Universiti Teknologi MARA for the 600-RMC/GIP 5/3 (009/2021) research funding and also for the facilities provided.

## REFERENCES

1. Varun, Sonam and Kakkara, R. (2019) Isatin and its derivatives: A survey of recent syntheses, reactions, and applications. *Medchemcomm*, **10(3)**, 351–368.

2. Abdul-Ghani, A. J. and Khaleel, A. M. N. (2009) Synthesis and characterization of New Schiff bases derived from N (1)-substituted isatin with dithiooxamide and their Co(II), Ni(II), Cu(II), Pd(II) and Pt(IV) complexes. *Bioinorganic Chemistry and Application*.

3. Kumar, R., Kumar, S. and Bala, M. (2020) Synthesis, characterisation and antibacterial activity of some indole derivatives and their inclusion complexes with β-cyclodextrin. *Oriental Journal of Chemistry*, **36**, 923–933.

4. Patil, S. A, Naik, V. H., Kulkarni, A. D. and Badami, P. S. (2010) Spectroscopic, DNA cleavage and antimicrobial studies of Co(II), Ni(II) and Cu(II) complexes of sulfur donor Schiff bases. *Journal of Sulfur Chemistry*, **31**, 109–121.

5. Marfak, F., Safitri, N. E., Putri, E. M. M., Pambudi, A. B. and Fadlan, A. (2020) Synthesis and Anticancer study of complex nickel (II) 5,7-dibromoisatin-derived hydrazine carbothiamide. *AIP Conference Proceedings*, **2237**.

6. Sulaiman, A. A., Zierkiewicz, W., Michalcyzk, M., Malik-Gajewska, M., Ahmad, S., Alhoshani, A., As Sobeai, H. M., Bieńko, D. and Isab, A. A. (2020) Synthesis, characterization, DFT optimization and anticancer evaluation of phosphanegold(I) dithiocarbamates. *Journal of Molecular Structure*. **1218**, 128486.

7. Xu, Z., Zhang, S., Chuan, G., Jing, F., Feng, Z., Lv, Z. -S. and Feng, L. -S. (2016) Isatin hybrids and their anti-tuberculosis activity. *Chinese Chemical Letters*, **28(2)**, 159–167.

8. Elsaman, T., Mohamed, M. S., Eltayib, E. M., Abdel Aziz, H. A., Abdalla, A. E., Munir, M. U. and Mohamed, M. A. (2022) Isatin derivatives as broad-spectrum antiviral agents: The current landscape. *Medicinal Chemistry Research*, **31**, 244–273.

9. Meleddu, R., Distinto, S., Corona, A., Tramontano, E., Bianco, G., Melis, C., Cottiglia, F. and Maccioni, E. (2017). Isatin thiazoline hybrids as dual inhibitors of HIV-1 reverse transcriptase. *Journal of Enzyme Inhibition and Medicinal Chemistry*, **32(1)**, 130-136.

10. Bonaccorso, C., Marzo, T. and La Mendola, D. (2019) Biological applications of thiocarbohydrazones and their metal complexes: A perspective review. *Pharmaceuticals*, **13(1)**, 4.

11. Satisha, M. P., Revankar, V. K. and Pai, K. S. R. (2007) Synthesis, structure, electrochemistry, and spectral characterization of bis-isatin thiocarbohydrazone metal complexes and their antitumor activity against ehrlich ascites carcinoma in Swiss albino mice. *Metal-Based Drugs*, **2008**, 362105.

12. Govindaraju, L., Jenarthanan, S., Subramanyam, D. and Ajitha, P. (2021) Antibacterial activity of various intracanal medicament against enterococcus faecalis, streptococcus mutans and staphylococcus aureus: An in vitro study. *Journal of Pharmacy and BioAllied Sciences*, **13**, S157–S161.

13. Tsipis, A. C. (2014). Retracted: DFT flavor of coordination chemistry. *Coordination Chemistry Reviews*, **272**, 1–29.

14. Delley, B. (2000) From molecules to solids with the DMol3 approach. *Journal of Chemical Physics*, **113**, 7756.

15. Ahmat, N., Wibowo, A., Syed Mohamad, S. A., Muhammad Low, A. L., Sufian, A. S., Muhd Yusof, M. I. and Latip, J. (2014) A new symmetrical tetramer oligostillbenoid containing tetrahydrofuran ring from the stem bark of *Dryobalanops lanceolata*. *Journal of Asian Natural Products Research*, **16(11)**, 1099–1107.

16. Khaidir, S. S., Bahron, H., Mohd Tajuddin, A. and Kurniawan, C. (2020) Synthesis of tetranuclear zinc(II) azomethine complex: A comparative appraisal between conventional and microwave assisted methods. *Malaysian Journal of Chemistry*, **22**, 120–125.

17. Ogutu, H. F. O., Saban, W., Malgas-Enus, R. and Luckay, R. C. (2020) Design, synthesis and spectroscopic characterization of mixed N- and O-donor Schiff base ligands ($N_2O_3$): Crystal structures of free ligands. *Journal of Molecular Structure*. **1211**, 128106.

18. Manan, M. F., Kassim, K. and Abdul Manan, M. A. F. (2012) Synthesis, characterization and conductivity studies of Schiff base ligand derived from isatin and O-phenylenediamine with its cobalt(II) metal complex and lithium-Schiff base compound. *The Malaysian Journal of Analytical Sciences*, **16**, 318–324.

19. Nasaruddin, N. H., Ahmad, S. N., Sirat, S. S., Wai, T. K., Zakaria, N. A. and Bahron, H. (2021) Structural characterization, DFT, Hirshfeld surface analysis and antibacterial activity of a Schiff base derived from cyclohexanediamine. *Journal of Molecular Structure*, **1232**, 130066.

20. Benedek, N. A., Snook, I. K., Latham, K. and Yarovsky, I. (2005) Application of numerical basis sets to hydrogen bonded systems: A density functional theory study. *The Journal of Chemical Physics*, **122**, 144102.

21. Yakan, H., Cavus, M. S., Zengin Kurt, B., Muglu, H., Sonmez, F. & Guzel, E. (2021) A new series of asymmetric bis-isatin derivatives containing urea/thiourea moiety: Preparation, spectroscopic elucidation, antioxidant properties and theoretical calculations. *Journal of Molecular Structure*, **1239**, 130495.

22. Cai, Y. Y., Xu, L. Y., Chai, L. Q. and Li, Y. X. (2020) Synthesis, crystal structure, TD/DFT calculations and Hirshfeld surface analysis of 1(4-((Benzo)dioxol-5-ylmethyleneamino)phenyl) ethanone oxime. *Journal of Molecular Structure*, **1204**, 127552.

23. Vijayaraj, R., Subramanian, V. and Chattaraj, P. K. (2009) Comparison of Global reactivity descriptors calculated using various density functionals: A QSAR perspective. *Journal of Chemical Theory and Computation*, **5**, 2744–2753.

24. Parr, R. G., Szentpa´ly, L. V. and Liu, S. B. (1999) Electrophilicity index. *Journal American Chemical Society*, **121**, 1922–1924.

25. Pearson, R. G. (2005) Chemical hardness and density functional theory. *Journal Chemical Science*, **117**, 369–377.

26. Domingo, L. R., Aurell, J. M., Perez, P. and Contreras, R. (2002) Quantitative characterization of the global electrophilicity power of common diene/dienophile pairs in diels±alder reactions. *Tetrahedron*, **58**, 4417–4423.

27. Acharya, D. and Dutta, T. K. (2021) Elucidating the network features and evolutionary attributes of intra- and interspecific protein–protein interactions between human and pathogenic bacteria. *Scientific Reports*. **11**, 190.